

Assessment of across-wind responses for aerodynamic optimization of tall buildings

Zhendong Xu^a and Jiming Xie^{*}

Zhejiang University, College of Civil Engineering and Architecture, Hangzhou 310058, China

(Received January 20, 2015, Revised September 16, 2015, Accepted September 20, 2015)

Abstract. A general approach of aerodynamic optimization of tall buildings is presented in this paper, focusing on how to best compromise wind issues with other design aspects in the most efficient manner. The given approach is reinforced by establishing an empirical method that can quickly assess the across-wind loads and accelerations as a function of building frequencies, building dimensions, aspect ratios, depth-to-width ratios, and site exposures. Effects of corner modifications, including chamfered corner and recessed corner, can also be assessed in early design stages. Further, to assess the effectiveness of optimization by tapering, stepping or twisting building elevations, the authors introduce a method that takes use of sectional aerodynamic data derived from a simple wind tunnel pressure testing to estimate reductions on overall wind loads and accelerations for various optimization options, including tapering, stepping, twisting and/or their combinations. The advantage of the method is to considerably reduce the amount of wind tunnel testing efforts and speed up the process in finding the optimized building configurations.

Keywords: tall building design; aerodynamic optimization; shape modifications; across-wind response; wind tunnel tests

1. Introduction

Development of modern high-rise buildings raises new challenges to structural engineers in their wind-resistant design. With increasing of building height and slenderness, the structural design of tall buildings is often found to be governed by across-wind responses that can be considerably higher than those initially predicted with conventional building code methods. It has also been found that across-wind responses tend to be more sensitive to a building's geometry than along-wind drags. These findings lead to an understanding that optimizing building shapes can efficiently reduce across-wind responses and result in significant monetary savings for tall building projects, especially for super-tall buildings (normally 300 m or taller) (Kwok 1988, Isyumov *et al.* 1989, Hayashida and Iwasa 1990, Irwin 2007, Xie 2012). The process of modifying building shapes to reduce wind responses is commonly referred to as "building aerodynamic optimization".

In engineering practice, the challenge of building aerodynamic optimization is often not about

^{*}Corresponding author, Professor, E-mail: jiming_xie@zju.edu.cn

^a Graduate student

whether an optimized shape can be found to reduce the wind loads to a satisfied level, but about whether an optimized configuration can be implemented without or at least with minimum impacts on other design aspects (Xie 2012). At conceptual or preliminary design stages, aerodynamic optimization is usually not within the scope of work because the potential across-wind response remains unknown due to lack of a reliable assessment method. A higher-than-expected across-wind response is often detected by wind tunnel tests after the completion of the preliminary design. However, at this design stage, building shape changes have become very difficult without considerable amount of re-designing. In the end, the structural engineers have to reinforce the building by enlarging its structural members to accommodate the high wind loads and motions at extra project expenses.

In the last couple of decades, although the importance of building shape optimization has been well recognized in the building design community, only a handful projects reached aerodynamic optimization design due to practical difficulties. The first difficulty is that at preliminary design stages, due to lack of a reliable assessment method, designers cannot determine whether the across-wind response would be an issue or not, so that the aerodynamic effects are normally given little attention. The second difficulty is that designers cannot assess the effectiveness of different aerodynamic options without substantial wind tunnel testing of all possible options. This type of wind tunnel testing is considered time consuming and expensive.

This paper presents a general approach for building aerodynamic optimization by focusing on how to best compromise wind issues with other design aspects in the most efficient manner. To assist the proposed approach, an empirical method is given to estimate across-wind responses of rectangular buildings at early design stages. With this method, building designers can conduct a quick calculation to estimate wind loads and accelerations as a function of building frequencies, building dimensions, aspect ratios, depth-to-width ratios, and site exposures. Effects of corner modifications, including chamfered corners and recessed corners, can also be assessed. To further assess the effectiveness of optimization by tapering, stepping or twisting building elevations, a practical method is introduced. This method is to use sectional aerodynamic data to estimate the reductions on wind loads and accelerations by tapering, stepping, twisting and their combinations. This method can considerably reduce the amount of wind tunnel testing efforts and speed up the process in finding optimized building configurations, in comparison with traditional wind tunnel methods.

2. General approach of aerodynamic optimization for across-wind responses

An efficient procedure of aerodynamic optimization should start with a simple question: is the shape optimization necessary for the given project? To answer this question, one needs to estimate the approximate magnitudes of wind loads and accelerations first. Generally speaking, because drag coefficients can be estimated with reasonable precision, it is relatively easier to conduct along-wind estimation than across-wind. Therefore whether across-wind loads are critical for design can be predicted by assessing the ratio between across-wind loads and along-wind loads. Experience with many super-tall building projects indicates that major design issues related to wind effects are mostly associated with excessive across-wind loads detected through wind tunnel testing (Gu and Quan 2004, Irwin 2007, Xie 2014).

One major difference between along-wind and across-wind loads is that along-wind loads are approximately proportional to wind speed squared while across-wind loads normally proportional

to wind speed with power 3 to 3.5. Since across-wind responses are mainly induced by vortex shedding, the dependence of across-wind loads on wind speed can be well described by a non-dimensional parameter, fB/U (often called “reduced frequency”) where f is the fundamental sway frequency of study building, B is the building width, and U is the reference mean wind speed. The increment of across-wind loads with wind speed tends to escalate when the reduced frequency approaches the building's Strouhal number. For a rectangular building, the Strouhal number is about 0.1. Fig. 1 shows the study results for rectangular buildings where the reference wind speed is taken at roof height (Xie and Xu 2014). It can be seen from the plots that when the reduced frequency approaches to 0.1, the across-wind loads can be more than double of the along-wind loads. However, when the reduced frequency is greater than 0.25, the across-wind loads become less significant in comparison with the along-wind loads. The plots also indicate that across-wind loads are more pronounced in open terrain than in built-up terrain. In other words, a designer needs to be more cautious about across-wind response for a building located in water front than if it is located in a city center. For rectangular buildings in a city center, if the reduced frequency reaches to 0.20 or higher, the across-wind response would usually not be an issue for design. Building aerodynamic optimization will have remarkable benefits when the reduced frequency is smaller than 0.15.

While across-wind responses are often the leading cause of high wind loads or accelerations, there are other sources that may also induce high loads or accelerations. Fig. 2 shows a typical case of high accelerations in along-wind and torsional directions (Xie and Irwin 2000). In addition to relatively flexible in these two directions, the exceptionally small depth-to-width ratio makes the generalized mass light compared to the generalized force and thus causes high dynamic response. Fig. 3 illustrates a typical case of wake buffeting caused by upwind tall buildings (Xie 2012). Understanding the causes of high response is essential in searching for solutions. For the case shown in Fig. 2, having openings through on the top portion of the building was found most effective while in Fig. 3 changing study building's shape offers little help in reducing wake buffeting response. Since wake buffeting is sensitive to the relative locations between the upwind and downwind buildings, a small relocation of the downwind building can lead to significant response reductions.

Before working on optimization options, one needs to review the existing constraints that may limit the use of certain aerodynamic measures. The most common constraint on shape changes is the potential conflict with overall architectural concept due to a very straightforward reason: no building is going to be built primarily for winds.

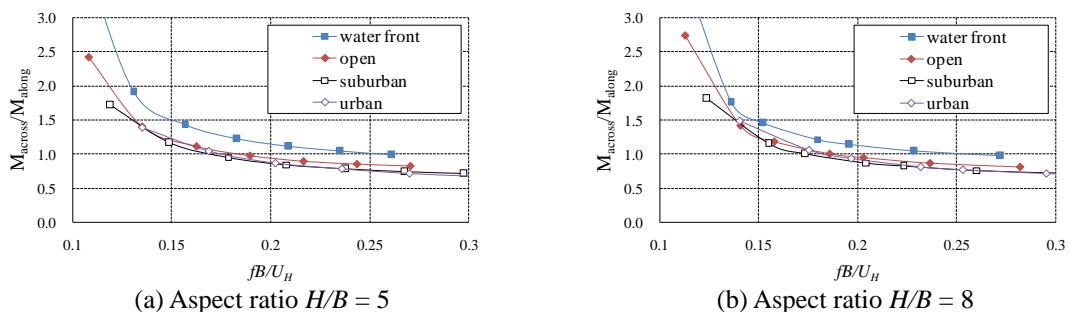


Fig. 1 Comparison of overturning moments in across-wind and along-wind directions

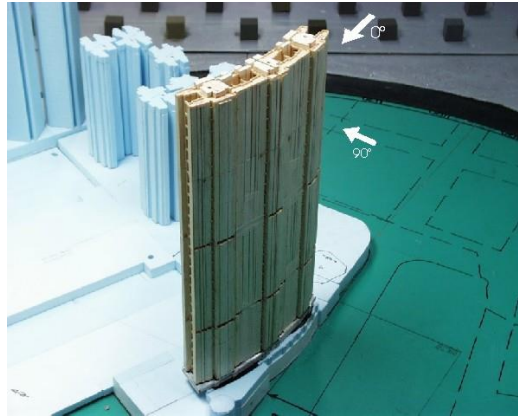


Fig. 2 Example of along-wind and torsion dominant case

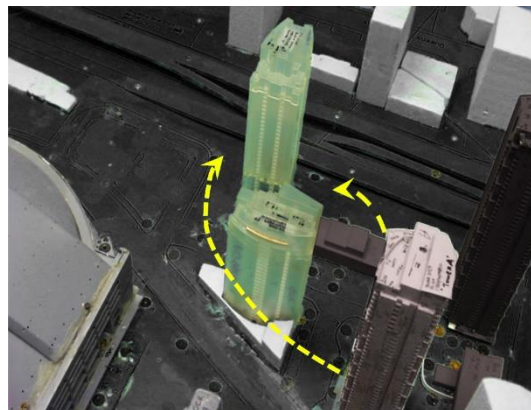


Fig. 3 Example of wake buffeting case

In the design of the project shown in Fig. 4, the twist angle from the base level to the roof level was taken as the key parameter for shape optimization (Xie *et al.* 2009). This parameter can considerably alter the aerodynamic behavior and wind responses, but does not significantly affect the overall architectural presentations. Fig. 5 shows a project where the shape of roof top sculpture was used for aerodynamic optimization (Xie 2012). The potential consequence of aerodynamic modifications on building height, structural system, cladding system, element vibration should be carefully reviewed to understand the practical constraints. In cold climate regions where winter snow is normal, any aerodynamic modifications that may cause sliding snow/ice built-up should be avoided.

On the bases of the above described studies, various options of aerodynamic optimization can then be examined. The objective is to compromise effectiveness of the feasible measures and the associated cost. Published wind tunnel results (Kwok and Isyumov 1998, Kareem *et al.* 1999, Tanaka *et al.* 2012) can be reviewed for this purpose. In general, optimization measures can be summarized into 5 categories (Xie 2014):



Fig. 4 Aerodynamic optimization by twisting



Fig. 5 Aerodynamic optimization by sculptured top

- 1) corner modifications;
- 2) tapering and stepping;
- 3) twisting;
- 4) opening;
- 5) sculptured top

The above described approaches of aerodynamic optimization can also be summarized by a 4-step procedure called SURE, where

- "S", the first step, stands for the abbreviation of "Specifying the objective of aerodynamic optimization", which includes the estimates of wind loads and building accelerations in comparison with preferred load capacity and relevant criterion. Based on these estimates, a specific objective of aerodynamic optimization can be established.
- "U", the second step, stands for "Understanding the causes of issues". If estimated wind loads are found to be excessive, an important investigation is to identify the cause(s). This basically determines the type of measures that would be effective for the given objective.
- "R", the third step, stands for "Recognizing the constraints of aerodynamic options", which requires a study of the project, appreciation of the architectural concept, anticipation of

potential consequences of shape changes, etc.

- “E”, the last step, stands for “Examining alternative options of configurations”. By analyzing feasibility, effectiveness and costs for each option, an optimized building configuration can be obtained. Usually, a wind tunnel testing is followed to confirm the wind response of the final building configuration.

In the following sections, assessment methods for across-wind response will be given. It should be noted that although across-wind response is the leading cause of high wind responses, other aerodynamic phenomena, such as wake buffeting, may also cause potential issues for design, as described before. These phenomena have been studied mainly for specific projects and the results cannot lead to general conclusions yet. Therefore, it is considered to be a good engineering practice for tall building designs to have a preliminary wind tunnel study on conceptual design schemes to identify potential problems before design development

3. Estimate method of across-wind responses

3.1 Mathematic model of across-wind responses

To carry on the above described optimization procedures, we need an estimate on potential across-wind loads so that we can determine if the shape modifications are necessary and, if necessary, how much reduction is needed from optimization.

Based on theory of random vibrations, the variance of modal acceleration to wind excitations can be given by

$$\sigma_{a_j}^2 \cong \frac{1}{M_j^2} \left(\int_0^\infty S_{F_j}(f) df + \frac{\pi f_j}{4\zeta_j} S_{F_j}(f_j) \right) \quad (1)$$

where M_j is the generalized mass, f_j the natural frequency; and ζ_j the structural damping ratio of the j -th mode. S_{F_j} is the generalized force spectrum. For simplicity, we replace the generalized force spectrum by its non-dimensional form $S_{F_j} = q_0 K_H B H S_{F_j}^*$; where q_0 is a reference design wind pressure, taken as 10-minute mean at 10m height in open terrain, K_H is the ratio between the mean wind pressure at building roof height on study site and the wind pressure at 10 m height in open terrain, B is the building's reference width, and H is the building height.

The first term in Eq. (1) represents the background contribution while the second term is the resonance. For cases of response being dominated by across-wind loads, the background contribution is normally less than 5%. Therefore the inertial load distributions due to across-wind response can be written as follows

$$P_R \cong q_0 K_H B H g_R \frac{m_z \varphi_j(z)}{M_j} \sqrt{\frac{\pi f_j}{4\zeta_j} S_{F_j}^*(f_j)} \quad (2)$$

where g_R is the peak factor for resonance, φ_j is the mode shape, and m_z is the floor mass at elevation z .

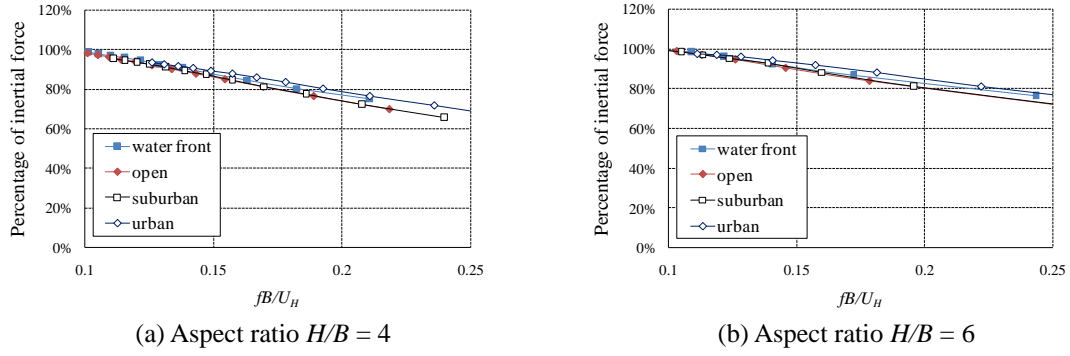


Fig. 6 Relative contributions of inertial force to overall base loads

The exposure factor K_H can be estimated by $K_H = (z_g/10)^{2\alpha_0} (H/z_g)^{2\alpha}$ where z_g is the gradient height in m, α_0 is power law exponent of mean wind speed profile over the standard open terrain, and α is the power law exponent of mean wind speed profile on study site.

The background fluctuating loads at elevation z can be generally expressed by

$$P_B(z) \cong q_0 K_H B h_z g_B \psi(z) C_F(z) J \quad (3)$$

where h_z is the floor height at elevation z , g_B is the peak factor for background, $\psi(z)$ represents the fluctuating load profile, $C_F(z)$ is the force coefficient, and J is the reduction factor due to lack of correlations of wind turbulence over the building height.

Fig. 6 shows the relative contributions of inertial force to overall dynamic base loads of square buildings. The results suggest that within the range of interest (typically $fB/U_H \leq 0.2$), the inertial contributions are far greater than background. Therefore, it is reasonable in practical application to make effective static load distributions being similar to inertial forces and approximate the contribution of background by incremental factors λ .

The practical model for across-wind loads is therefore written by the following expression

$$P_k(z) \cong q_0 \left(K_H \frac{m_z}{M_j} \frac{H}{h_z} \varphi_j(z) \right) \left(\frac{g_R}{\sqrt{\zeta_j}} \sqrt{\frac{\pi f_j}{4} S_{F_j}^{**}(f_j) \lambda} \right) \mu_{sH} \cdot B_z h_z \quad (4)$$

where a new factor, μ_{sH} , is introduced to further normalize the peaks of force spectra, i.e., to make $S_{F_j}^* = \mu_{sH}^2 S_{F_j}^{**}$. In this way, the effects of building configurations on their force spectra can be separated into two portions: changes of peak amplitudes and changes of energy distributions.

To make it convenient for application, Eq. (4) is simplified to have a code-type format.

$$P_k(z) = (q_0 \mu_{zH} \mu_{sH} \beta_H) \cdot B_z h_z \quad (5)$$

where

$$\mu_{zH} = K_H \left(\frac{m_z}{M_j} \frac{H}{h_z} \right) \varphi_j(z) = \text{distribution factor of across-wind loads at elevation } z;$$

μ_{sH} = across-wind force coefficient;

$$\beta_H = \frac{g_R}{\sqrt{\zeta_j}} \sqrt{\frac{\pi f_j}{4} S_{F_j}^{**}(f_j) \lambda} = \text{across-wind dynamic factor.}$$

The coefficients involved in Eq. (5) are determined based on the results of wind tunnel tests and data fitting (GB50009-2012, Quan and Gu 2006) and are given in Sections 3.2 and 3.3.

For the estimate of across-wind accelerations, the following approximate equation can be used.

$$a_k(z) = \frac{P_k(z)}{m_z} \quad (6)$$

3.2 Across-wind force coefficient μ_{sH}

The across-wind force coefficient is expressed by

$$\mu_{sH} = C_H C_m \quad (7)$$

where C_H is the basic force coefficient for rectangular shape and is a function of the depth-to-width ratio.

The corner modification factor C_m equals 1.0 for unmodified building section and takes a value smaller than 1.0 for modified corners. Based on the recommendations given by the Chinese building code (GB50009-2012), corner modification factors are shown in Fig. 7 as a function of b/B . Please note that modified corners not only reduce the amplitude of vortex shedding as specified by factor C_m , but also change the energy distribution in force spectrum which will be further accounted in the calculation of dynamic factors.

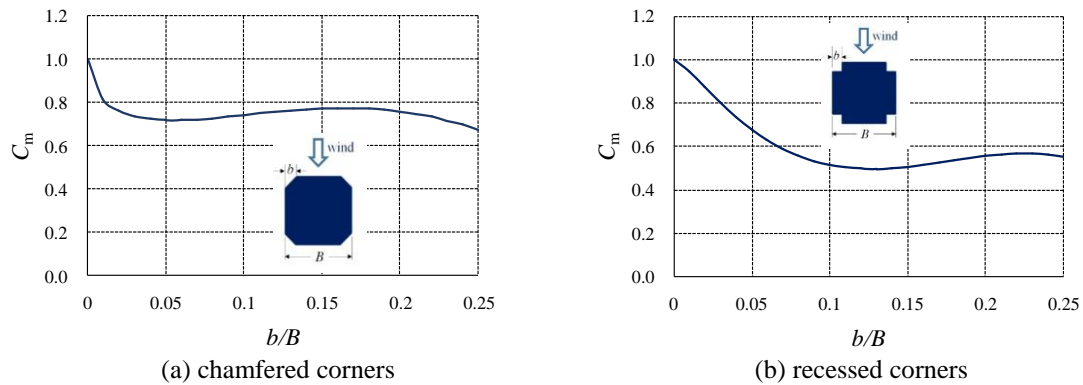


Fig. 7 Reduction factor C_m for modified corners

Table 1 Basic force coefficient, C_H

Ratio D/B	0.5	0.75	1	1.25	1.5	1.75	2
C_H	1.15	1.01	0.93	0.87	0.82	0.79	0.76

3.3 Across-wind dynamic factor β_H

The across-wind dynamic factor is expressed in the following practical format

$$\beta_H = \frac{g_R}{\sqrt{\zeta}} \sqrt{S_R} \lambda_E \lambda_{DB} \lambda_{HB} \lambda_{sm} \quad (8)$$

It is suggested to take damping ratio $\zeta=2\%$ as a preliminary estimate. The peak factor g_R is typically between 2.5 and 3.5, the lower value for severer vortex-induced across-wind responses. The standard spectrum $\sqrt{S_R}$ is taken from the measurements of a square building with $H/B=6$ in open terrain. The deviations from the standard spectrum due to different site exposures, depth-to-width ratios D/B , aspect ratios H/B are compensated by the modification factors, as given in Fig. 8 and Tables 2 through 5.

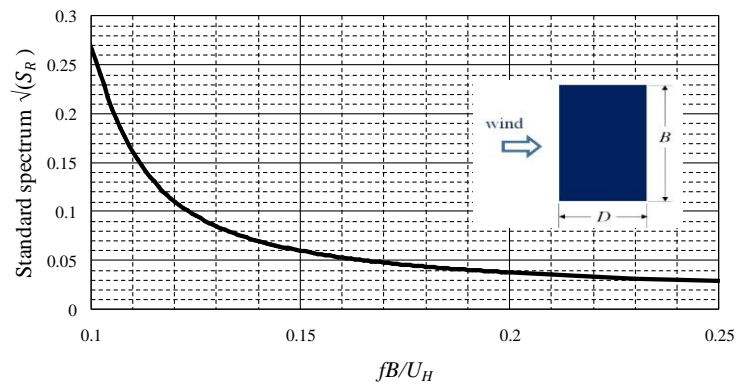


Fig. 8 Standard across-wind force spectrum

Table 2 Modification factors for exposure, λ_E

Exposure	fB/U_H											
	0.1	0.11	0.12	0.13	0.14	0.15	0.16	0.17	0.18	0.19	0.2	0.25
A	1.24	1.25	1.22	1.21	1.21	1.21	1.21	1.22	1.22	1.23	1.23	1.23
B	1.00	1.00	1.00	1.00	1.00	1.00	1.00	1.00	1.00	1.00	1.00	1.00
C	0.85	0.93	0.97	0.98	0.99	0.99	0.99	0.98	0.98	0.97	0.97	0.97
D	0.71	0.92	1.06	1.12	1.15	1.16	1.16	1.15	1.14	1.13	1.12	1.12

where

- A: Water front with mean speed power law exponent $\alpha=0.11$;
 B: Open terrain with mean speed power law exponent $\alpha=0.15$;
 C: Suburban terrain with mean speed power law exponent $\alpha=0.22$;
 D: Urban terrain with mean speed power law exponent $\alpha=0.30$.

In summary, the procedure of across-wind load estimates can be conducted following the flow chart as below.

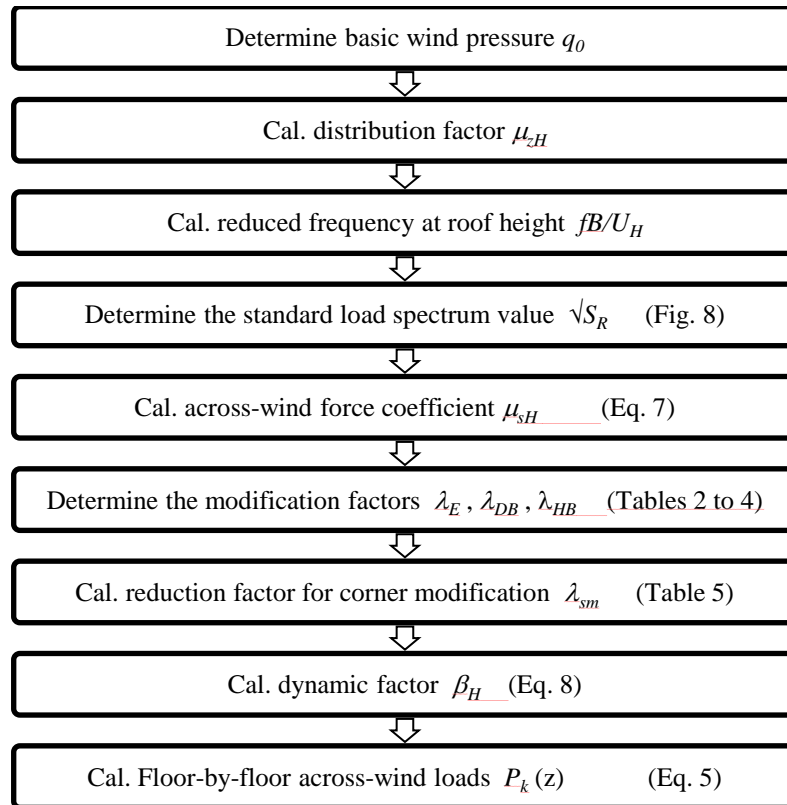


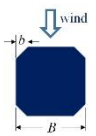
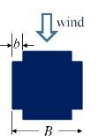
Table 3 Modification factors for depth-to-width ratio, λ_{DB}

D/B	fB/U_H											
	0.1	0.11	0.12	0.13	0.14	0.15	0.16	0.17	0.18	0.19	0.2	0.25
0.50	0.13	1.29	0.63	0.44	0.40	0.39	0.40	0.41	0.43	0.45	0.47	0.59
0.75	0.89	1.17	0.90	0.82	0.79	0.78	0.78	0.78	0.79	0.80	0.80	0.85
1.00	1.00	1.00	1.00	1.00	1.00	1.00	1.00	1.00	1.00	1.00	1.00	1.00
1.25	0.80	0.92	1.01	1.06	1.09	1.10	1.11	1.11	1.11	1.11	1.11	1.08
1.50	0.69	0.86	0.99	1.07	1.12	1.14	1.16	1.16	1.17	1.16	1.16	1.13
1.75	0.62	0.81	0.96	1.06	1.12	1.16	1.18	1.19	1.19	1.20	1.19	1.16
2.00	0.58	0.77	0.94	1.05	1.12	1.16	1.19	1.21	1.22	1.22	1.22	1.19

Table 4 Modification factors for aspect ratio, λ_{HB}

H/B	fB/U_H											
	0.1	0.11	0.12	0.13	0.14	0.15	0.16	0.17	0.18	0.19	0.2	0.25
4	0.60	0.73	0.81	0.86	0.89	0.92	0.94	0.96	0.98	1.00	1.03	1.15
5	0.83	0.92	0.99	1.03	1.06	1.08	1.11	1.14	1.16	1.19	1.22	1.38
6	1.00	1.02	1.04	1.06	1.09	1.11	1.14	1.16	1.19	1.22	1.25	1.43
7	1.14	1.09	1.06	1.06	1.08	1.10	1.12	1.14	1.17	1.20	1.23	1.41
8	1.23	1.16	1.07	1.05	1.05	1.05	1.07	1.09	1.11	1.13	1.16	1.32

Table 5 Modification factors for corner modifications, λ_{sm}

	Exposure	b/B	fB/U_H						
			0.1	0.125	0.15	0.175	0.2	0.225	0.25
	A&B	5%	0.428	0.951	1.095	1.095	1.095	1.095	1.049
		10%	0.265	0.591	0.754	0.808	0.827	0.819	0.808
		20%	0.326	0.950	0.976	0.905	0.862	0.817	0.791
	C	5%	0.525	0.909	1.030	1.038	1.035	1.029	0.999
		10%	0.404	0.653	0.783	0.824	0.836	0.827	0.818
		20%	0.472	0.969	0.982	0.925	0.890	0.858	0.841
	D	5%	0.607	0.865	0.960	0.977	0.971	0.958	0.947
		10%	0.506	0.710	0.812	0.840	0.844	0.835	0.828
		20%	0.582	0.987	0.988	0.946	0.917	0.897	0.889
	A&B	5%	0.326	0.771	0.990	1.000	1.000	1.000	1.000
		10%	0.182	0.477	0.671	0.752	0.781	0.777	0.771
		20%	0.205	0.918	0.750	0.672	0.649	0.632	0.632
	C	5%	0.432	0.768	0.954	0.989	0.997	0.998	0.996
		10%	0.249	0.494	0.672	0.752	0.782	0.786	0.782
		20%	0.325	0.948	0.782	0.699	0.669	0.651	0.653
	D	5%	0.517	0.766	0.916	0.977	0.993	0.995	0.992
		10%	0.302	0.511	0.672	0.753	0.783	0.796	0.792
		20%	0.411	0.977	0.812	0.726	0.689	0.669	0.673

4. Assessment method of aerodynamic effectiveness

While the above method can be used to estimate the effects of corner modifications, it cannot predict the effects of aerodynamic optimization that involves tapering, stepping or twisting building elevations, the three common schemes in super-tall building design.

To include these common schemes in the examination for alternative options during Step 4 of the aerodynamic optimization, a practical method has been developed to assess the effectiveness of

building tapering, stepping or twisting with minimum amount of wind tunnel tests (Xie 2014). The method can be illustrated by Fig. 9.

The wind tunnel testing on original configuration shown in Fig. 9 is to measure the sectional aerodynamic force coefficients and calculate their spectra. Based on strip assumption, the generalized force of the original configuration can be calculated by following integration.

$$S_{j0}(f) = (q_0 B_0 H)^2 \iint (V_{q1} \varphi_{j1}) (V_{q2} \varphi_{j2}) \sqrt{S_\theta(K_1) S_\theta(K_2)} \exp \left[-c \frac{K_1 + K_2}{2} \left| \frac{z_1 - z_2}{B_0} \right| \right] dz_1^* dz_2^* \quad (9)$$

where q_0 is the reference wind pressure, subscripts 1 and 2 refer to elevation z_1 and z_2 , respectively; S_θ = across-wind force coefficient spectrum at elevation z from direction θ in reference to local orientation; $K_{1,2} = f B_{1,2} / U_{1,2}$; $z^* = z / H$; and c = coherence factor.

To assess the effectiveness of building tapering, stepping and twisting, a similar approach can be used to calculate the generalized force coefficient spectrum of the modified building based on the local width and orientation at each elevation. The ratio of the generalized force coefficient spectra between the modified building configuration and the original configuration provides an index of the effectiveness, i.e.

$$E(f_j) = \frac{\iint (V_{q1} V_{B1} \varphi_{j1}) (V_{q2} V_{B2} \varphi_{j2}) \sqrt{S_{\theta1}(K_1) S_{\theta2}(K_2)} \exp \left[-c \frac{K_1 + K_2}{2} \left| \frac{z_1}{B_1} - \frac{z_2}{B_2} \right| \right] dz_1^* dz_2^*}{\iint (V_{q1} \varphi_{j1}) (V_{q2} \varphi_{j2}) \sqrt{S_\theta(K_1) S_\theta(K_2)} \exp \left[-c \frac{K_1 + K_2}{2} \left| \frac{z_1 - z_2}{B_0} \right| \right] dz_1^* dz_2^*} \quad (10)$$

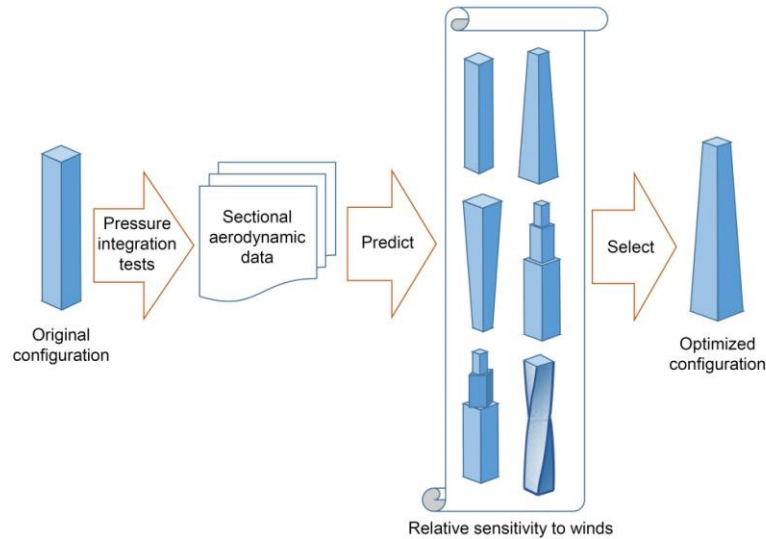


Fig. 9 Illustration of the proposed method for effectiveness assessment

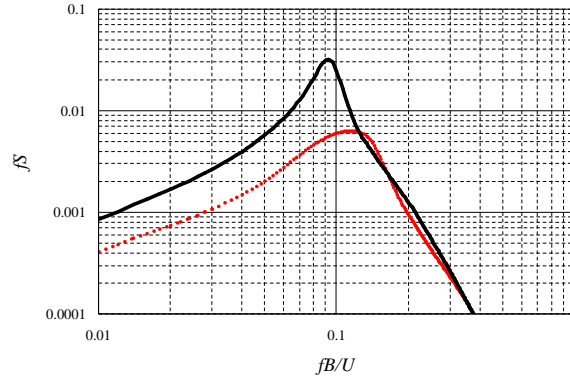
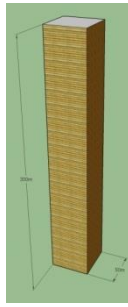


Fig. 10 Effectiveness of tapering on across-wind force



Basic building information:

$H=300$ m; $B=50$ m

Building mass density = 300 kg/m^3

Fundamental frequency $f=0.15$ Hz

Mode shape $\varphi_j(z) = (z/H)^{1.3}$

Damping ratio $\zeta=0.02$

Basic design wind pressure $q_0=0.65$ kPa, which is defined as 10-minute mean at 10 m height in a standard open terrain ($\alpha=0.15$)

Exposure category: open terrain

Fig. 11 Study building

5. Illustrating example

To illustrate the proposed procedure of S.U.R.E., a study of a typical square building shown in Fig. 11 is demonstrated.

Step 1: Specifying the objective of aerodynamic optimization

In this step, a preliminary estimate of overall wind loads is needed to assess the necessity of aerodynamic optimization for this project.

The along-wind loads can be readily estimated with most building codes, and in this case the along-wind base shear and overturning moment are calculated to be $S_{along}=4.21 \times 10^4$ kN and $M_{along}=7.64 \times 10^6$ kN-m, respectively.

To estimate the across-wind loads, the method described in Section 3 of this paper is utilized. The reader can refer to the flow chart shown in Section 3 for step-by-step procedures.

- Calculate the distribution factor μ_{zH}
- Calculate reduced frequency at roof height

$$K_H = (300/10)^{2 \times 0.15} = 2.77$$

Table 7 Example: Calculation of distribution factor μ_{zH} of across-wind loading

Floor	z (m)	h_z (m)	B (m)	z_H	P (kN)
1	0.0	7.5	50.0	0.000	0.00
2	7.5	4.5	50.0	0.083	18.32
3	12.0	4.5	50.0	0.153	33.75
4	16.5	4.5	50.0	0.232	51.05
5	21.0	4.5	50.0	0.317	69.85
...	Similar calculations omitted here				
63	282.0	4.5	50.0	9.285	2044.59
64	286.5	4.5	50.0	9.478	2087.11
65	291.0	4.5	50.0	9.672	2129.82
66	295.5	4.5	50.0	9.867	2172.74
Roof	300.0			sum	6.31E+04

Step 2: Understanding the cause of issues

The results of the above estimates indicate that the wind-resistant design of the study building will be governed by across-wind dynamic responses. Therefore the objective of the aerodynamic optimization is mainly to minimize the across-wind responses.

Step 3: Recognizing the constraints of aerodynamic measures

For illustration purpose, we assume that only tapering-type modifications are acceptable from architectural point of view. Certainly, the potential effects on across-wind responses largely depend on the detailed parameters of tapering and the optimization is basically to optimize these parameters. Conventional approach is to fabricate many building models with various tapering parameters and determine the optimized parameters through substantial wind tunnel tests. This conventional approach is considered time consuming and expensive. Comparatively, the new approach proposed in Section 4 of the paper requires much less wind tunnel work and can be used as a practical tool for this purpose. For the given example, it's only required to have one simple pressure model testing to measure the sectional aerodynamic force spectrum, as shown in Fig. 12. Then by using Eq. (10), the optimized parameters can be found by comparing the wind loading reduction factors for various sets of tapering parameters. The reduction factor is taken to be the square root of the effectiveness index determined by Eq. (10).

Step 4: Examining alternative options of configurations

In addition to tapering, its variations can also be examined as alternative options. Fig. 13 shows the wind loading reductions for different tapering ratios as well as two variations: tapering on upper portion only and upper portion stepping. Tapering ratio is defined by decrement in building width per unit height.

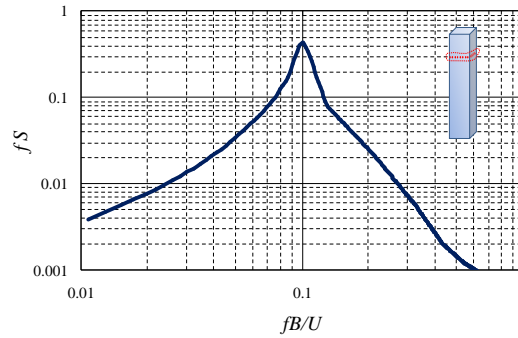


Fig. 12 Illustration of sectional across-wind load spectrum

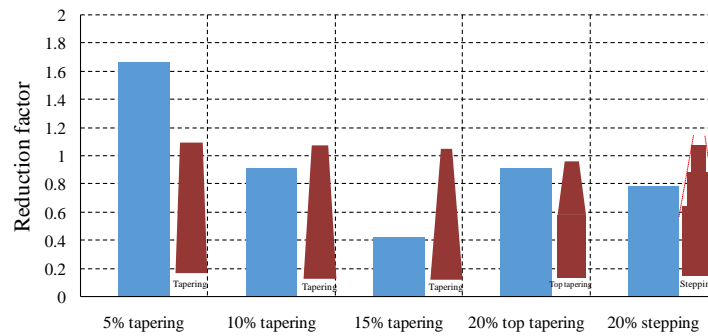


Fig. 13 Wind loading reduction factors

The results shown in Fig. 13 suggest that small tapering may result in negative benefits, caused by peak of wind loading energy shifting to higher reduced frequency region, leading to localized increase of wind loading spectrum. Detailed explanations for this phenomenon can be found in a paper by Xie (2014).

It should be emphasized that the described procedure S.U.R.E. is to practically assist the aerodynamic optimizations. While the methods given in Section 3 and Section 4 provide useful guidance for aerodynamic optimizations, the results from these methods contain simplifications and are therefore approximate. In particular, the complicated surrounding effects and 3-D flow effects are not considered. Therefore after reaching an optimized building geometry with these methods, a confirmation wind tunnel testing is necessary to validate the conclusions.

6. Conclusions

A general approach of aerodynamic optimization is presented in this paper, which consists of four major steps S.U.R.E, abbreviating the procedures of “Specifying the objective of aerodynamic optimization”, “Understanding the causes of issues”, “Recognizing the constraints of aerodynamic

measures”, and “Examining alternative options of configurations”. The focus of this approach is to compromise the wind issues with other design aspects in the most efficient manner.

To assist the proposed aerodynamic optimization approach, an empirical method is established to estimate the across-wind response of rectangular buildings at early design stages. With this method, building designers can do a quick calculation to estimate across-wind loads and accelerations as a function of building frequencies, building dimensions, aspect ratios, depth-to-width ratios, and site exposures. Effects of corner modifications, including chamfered corner and recessed corner, can also be assessed.

To assess the effectiveness of optimization by tapering, stepping or twisting building elevations, a practical method is further introduced. This method is to use the sectional aerodynamic data derived from a preliminary wind tunnel testing to estimate the reductions of wind loads and accelerations by tapering, stepping, twisting and their combinations. In comparison with the traditional wind tunnel approaches, this method can considerably reduce the amount of wind tunnel testing efforts and speed up the process in finding optimized building configurations.

References

- Gu, M. and Quan Y. (2004), “Across-wind loads of typical tall buildings”, *J. Wind Eng. Ind. Aerod.*, **92**(13), 1147-1165.
- Hayashida, H. and Y. Iwasa (1990), “Aerodynamic shape effects of tall building for vortex induced vibration”, *J. Wind Eng. Ind. Aerod.*, **33**(1-2), 237-242.
- Isyumov, N., Dutton, R. and Davenport, A.G. (1989), “Aerodynamic methods for mitigating wind-induced building motions”, *Proceedings of the Structures Congress*, ASCE.
- Irwin, P.A. (2007), “Wind engineering challenges of the new generation of super-tall buildings”, *Proceedings of the 12th Int. Conf. on Wind Eng.*, Cairns, Australia.
- Kareem, A., Kijewski, T. and Tamura, Y. (1999), “Mitigation of motion of tall buildings with recent applications”, *Wind Struct.*, **2**(3), 201-251.
- Kwok, K.C.S. (1988), “Effect of building shape on wind-induced response of tall buildings”, *J. Wind Eng. Ind. Aerod.*, **28**(1-3), 381-390.
- Kwok, K.C.S. and Isyumov, N. (1998), “Aerodynamic measures to reduce the wind-induced response of buildings and structures”, *Proceedings of the Structures Congress*, ASCE.
- National Standard of China (2012), *Load code for the design of building structures GB50009-2012*.
- Quan, Y. and Gu, M. (2006), “Analytical method of across-wind response and equivalent static wind loads of high-rise buildings”, *J. Eng. Mech. China* (in Chinese), **23**(9), 84-88.
- Tanaka, H., Tamura, Y., Ohtake, K., Nakai, M. and Kim, Y.C. (2012), “Experimental investigation of aerodynamic forces and wind pressures acting on tall buildings with various unconventional configurations”, *J. Wind Eng. Ind. Aerod.*, **107-108**, 179-191.
- Xie, J. and Irwin, P.A. (2000). “Key factors for torsional wind response of tall buildings”, *Proceedings of the 2000 Structures Congress*, ASCE.
- Xie, J. et al. (2009), *Wind engineering studies for Shanghai Center Tower, Report of Rowan Williams Davies & Irwin Inc.*
- Xie, J. (2012), “Aerodynamic optimization in super-tall building designs”, Keynotes, *Proceedings of the 7th International Colloquium on Bluff Body Aerodynamics and Its Applications*, Shanghai, China.
- Xie, J. (2014), “Aerodynamic optimization of super-tall buildings and its effectiveness assessment”, *J. Wind Eng. Ind. Aerod.*, **130**(7), 88-98.
- Xie, J. and Xu, Z. (2014), “Improvement of code calculations for across-wind loads”, *Proceedings of the 23rd National Conference of High-rise Buildings* (in Chinese), Guangzhou, China.